

Perfluoroalkanes in Water: Experimental Henry's Law Coefficients for Hexafluoroethane and Computer Simulations for Tetrafluoromethane and Hexafluoroethane

Rui P. Bonifácio, Agílio A. H. Pádua, and Margarida F. Costa Gomes*

Laboratoire de Thermodynamique des Solutions et des Polymères, UMR6003, Université Blaise Pascal/C.N.R.S., 24 Avenue des Landais, 63177 Aubière, France

Received: February 15, 2001; In Final Form: May 29, 2001

The solubility of hexafluoroethane in water was determined experimentally and, together with that of tetrafluoromethane, calculated by molecular simulation. A high-precision apparatus based on an extraction method was used to measure the solubility of hexafluoroethane in water in the temperature range of 287–328 K at pressures close to atmospheric. The experimental data obtained were used to calculate Henry's law coefficients $H_{2,1}(p_1^{\text{sat}}, T)$, whose temperature dependence was represented by appropriate correlations. The imprecision of the results was characterized by average deviations of $H_{2,1}$ from these smoothing equations and is of $\pm 0.17\%$. From the temperature variation of the Henry's law coefficients, partial molar solution quantities such as the variation of the Gibbs energy, enthalpy, entropy, and heat capacity were derived. Monte Carlo simulations, associated with Widom's test particle insertion method and the finite-difference thermodynamic integration technique, were used to calculate the residual chemical potential of low molecular weight alkanes and perfluoroalkanes in water leading to Henry's law coefficients. Simulations were performed from 280 to 500 K along the saturation line of the pure solvent. The simulation method was validated by the calculation of $H_{2,1}(p_1^{\text{sat}}, T)$ for methane and ethane in water for which quantitative predictions were attained even at the lowest temperatures. The calculations for tetrafluoromethane and hexafluoroethane in water were compared with experimental values, when available, to test intermolecular potential models. Solute-solvent radial distribution functions were obtained from simulation at low and high temperatures.

Introduction

Systems consisting of fully or partially fluorinated organic molecules are relevant for a wide variety of fields ranging from materials science to medicine. Recent applications of fluorinated hydrocarbons include the search for effective surfactants in supercritical solvents, namely, supercritical carbon dioxide,¹ and their utilization as artificial blood substitutes or as environmental probes to determine the exchanges between the atmosphere and natural waters.^{2,3}

Solubility measurements often constitute a significant source of information about the properties and structure of aqueous solutions,⁴ especially in the case of very dilute solutes for which calorimetric determinations are very difficult. Precise solubility measurements covering large ranges of temperature are frequently the sole means of obtaining the enthalpy and heat capacity changes associated with the dissolution process. Experimental information concerning the solubility in water of fully fluorinated hydrocarbons is scarce. This is due to their extremely low solubility which renders experiments particularly difficult.⁵

The present paper concerns, on one hand, the experimental determination with high precision of the solubility of hexafluoroethane in water, in a sufficiently large temperature range to allow an accurate calculation of the thermodynamic quantities associated with the dissolution. On the other hand, molecular simulation was used to calculate the Henry's law coefficients of low molecular weight alkanes and perfluoroalkanes in water.

This study provides an extension of the thermodynamic conditions already covered experimentally as well as access to microscopic details such as the structure of the solution, which are otherwise not easily obtainable.

It was observed experimentally that the solubility of low molecular weight perfluoroalkanes in water is 1 order of magnitude smaller than that of the corresponding alkanes. Molecular simulation seems an interesting tool to verify this behavior and to observe if the nonmonotonic trend of solubility with temperature along the saturation line of the solvent is reproduced.

Molecular simulation studies of fully fluorinated hydrocarbons are infrequent in comparison to those involving their hydrocarbon counterparts, possibly because of the lack of a simple and transferable intermolecular potential model.⁶ Hydrocarbons are commonly treated within the united-atom framework, according to which the methane molecule and the methyl and methylene groups are considered as single sites interacting through a potential such as the Lennard-Jones function.^{7,8} Some studies are reported in the literature where fluorocarbons are treated with all atoms explicit,⁹ a choice that involves a significant computational overhead. Recently, Cui et al.⁶ have proposed united-atom models for perfluoroalkanes that reproduce successfully the pure-fluid vapor-liquid equilibria for C_nF_{2n+2} with n ranging from 5 to 16. In the present work, we test the adequacy of a united-atom representation of small perfluoroalkanes for the calculation of properties in aqueous solution that depend on solute-water interactions.

A treatment of the solubility of gases in liquids and the structure of the resulting solutions using statistical mechanics

* To whom correspondence should be addressed. Fax: +33 4 73 40 71 85. E-mail: margarida.c.gomes@univ-bpclermont.fr.

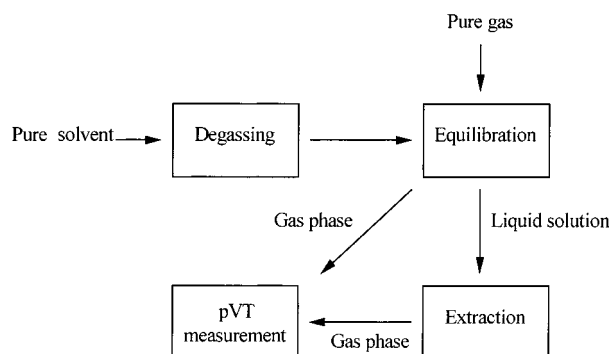


Figure 1. Block diagram of the experimental procedure used for solubility measurements.

calculations is feasible at present. Molecular simulations can be carried out, and in the cases where rigorous intermolecular potential models are available, quantitative predictions of solubility are possible, especially for systems involving small solutes. This has recently been done for methane and ethane in water using Monte Carlo simulations coupled with the test particle insertion method.¹⁰ The case of perfluoroalkanes having the same number of carbon atoms seems an interesting problem: not only the solubility of the latter species in water is lower than that of the normal alkanes but their molecular size is considerably greater, rendering the calculation of the chemical potential more difficult.

Experimental Section

Materials. The samples of hexafluoroethane used were supplied by Air Liquide, ultrahigh purity grade, with 99.95% mol/mol minimum stated purity. The gas was used as received from the manufacturer, and no further analysis was done to confirm the purity.

The sample of water used as solvent was three-times distilled in an all quartz system. The purity of the water was checked by measuring its conductivity using a CDM 92 conductivity meter from Radiometer. The samples used for the present measurements showed a resistivity greater than $10^6 \Omega \text{ cm}$.

Apparatus and Operation. The experimental equipment used in the present work was described in detail in a previous publication.¹¹ It makes use of an extraction technique originally developed by Benson and Krause^{12,13} and extensively used by Battino and co-workers.^{14–17} The solubility of a gaseous solute in a liquid solvent is determined by quantitatively extracting the gas present in the saturated solution at a given temperature and pressure.

The flow diagram of the solubility apparatus is shown in Figure 1. Before starting the dissolution process, the pure solvent is degassed following the procedure described by Battino and co-workers,¹⁸ with the residual gas dissolved in water after degassing being estimated as less than 0.001% of the saturation value at room temperature and atmospheric pressure. The saturation of pure water by the gaseous solute is attained in an equilibration cell similar to that described in detail by Benson and Krause.¹³ During the equilibration process (24–48 h, depending on the state point), the cell is maintained at constant temperature, to within $\pm 2 \text{ mK}$, inside a double-layer, 500 L, precision water thermostat (by means of PID controllers from TRONAC Inc., model PTC-40). Equilibrium temperatures are determined with a resolution of 1 mK with a Rosemount 25 Ω platinum resistance thermometer calibrated by the National Institute of Standards and Technology, U.S.A., coupled to a Leeds and Northrup Mueller bridge. The thermometer was

regularly checked in triple-point-of-water cells and in an NIST-certified benzoic acid cell. Temperatures are known with an accuracy of $\pm 20 \text{ mK}$.

Gas-phase and liquid-phase samples of the saturated solution are analyzed in order to determine precisely the amount of dry gas present. For this, known volumes of both phases (calibrated with a maximum imprecision of 0.01%) are isolated, and the amounts of solute are determined by measuring pressure, temperature, and volume of pure gas transferred into a manometric system.¹¹ Pressure is read using a Ruska quartz spiral manometer type XR-38 with a stated imprecision of $\pm 0.003\%$ and an estimated inaccuracy of $\pm 0.01\%$ regularly checked against a gas-lubricated dead weight gage (Ruska model 2465) with traceability of calibration to the National Institute Standards and Technology, U.S.A. The temperature of the manometric system and of the connecting glass and metal lines and of the manometer itself is controlled, at approximately $(40 \pm 0.005)^\circ\text{C}$, using a circulating water thermostat. The imprecision of the pVT analysis is at most $\pm 0.03\%$ of the amount of gaseous solute present in each phase.

Data Reduction. The method of data reduction used is thermodynamically rigorous and was reported in a previous publication.¹¹ The solubility will be expressed in terms of the Henry's law constant which can be defined as¹⁹

$$H_{2,1}(p,T) = \lim_{x_2 \rightarrow 0} \left[\frac{f_2(p,T,x_2)}{x_2} \right] \quad (1)$$

or equivalently¹⁹

$$H_{2,1}(p,T) = H_{2,1}(p_1^{\text{sat}},T) \exp \int_{p_1^{\text{sat}}}^p \frac{V_2^\infty(p,T)}{RT} dp \quad (2)$$

where f_2 and x_2 are the fugacity and molar fraction of component 2 (taken here to be the gaseous solute) in the solution, respectively, and V_2^∞ is the partial molar volume of the solute at infinite dilution.

The molar fraction of the gaseous solute in the liquid solution can be calculated from experimentally measured quantities:

$$x_2^L = \frac{n_2^L V_1^0(T)}{n_2^L [V_1^0(T) - V_2^\infty(p,T)] + V_{\text{LPB}}} \quad (3)$$

where V_{LPB} is the precisely known volume¹¹ of the liquid solution analyzed by the pVT measurement and V_1^0 the orthobaric molar volume of the solvent. The quantity n_2^L is the amount of dry gas present in the liquid solution which is determined by the pVT analysis in the manometric system (MS):

$$n_2^L = \frac{1}{RZ_2(p,T)} \left(\frac{pV}{T} \right)_{\text{MS}} \quad (4)$$

where Z_2 is the compressibility factor of the gaseous solute at the temperature and pressure of the manometric system.

The amount of the solute in the gaseous phase in equilibrium with the liquid solution, n_2^G , is also determined from a pVT analysis, with its molar fraction being given by

$$y_2 = n_2^G \frac{RTZ_{1,2}(p,T)}{pV_{\text{VPB}}} \quad (5)$$

where V_{VPB} is the precisely known volume¹¹ of the gaseous phase analyzed and $Z_{1,2}$ the compressibility factor for the binary gaseous mixture.

TABLE 1: Experimental Values for Henry's Law Coefficient of Hexafluoroethane in Water from 287 to 328 K

T/K	$x_2/10^{-7}$	p/MPa	$H_{2,1}(p^{\text{sat}}, T)/\text{GPa}$
287.704	16.42	0.0966	56.99
293.424	11.24	0.0890	76.12
298.464	9.975	0.0961	91.83
303.710	8.644	0.0980	106.84
308.606	8.303	0.1061	119.10
313.743	7.085	0.1010	130.02
318.436	7.232	0.1103	137.02
323.540	7.011	0.1143	142.80
328.238	7.033	0.1205	146.46

Considering the usual definition for the fugacity of component 2,¹⁹ Henry's law coefficient can be calculated from

$$H_{2,1}(p, T) = \lim_{x_2 \rightarrow 0} \left[\frac{n_2^{\text{G}} RT n_2^{\text{L}} [V_1^0(T) - V_2^{\infty}(p, T)] + V_{\text{LPB}}}{n_2^{\text{L}} V_1^0(T) V_{\text{VPB}}} \times \phi_2(p, T) Z_{12}(p, T) \right] \quad (6)$$

where ϕ_2 is the fugacity coefficient of the solute. The values of V_{VPB} and V_{LPB} are corrected for the different temperatures using appropriate thermal expansion coefficients.¹¹

Although the equilibrium pressure is not explicitly present in eq 6, it is required for the determination of the product $\phi_2 Z_{12}$ (normally close to unity). The equilibrium pressure is calculated by an iterative procedure starting with an initial guess for the pressure given by application of Raoult's law. The iterations converge rapidly and give coherent values for the equilibrium pressure and for the fugacity coefficient.

Experimental Results. Temperatures are reported on the ITS-90 scale. The relative atomic masses used were taken from the IUPAC tables,²⁰ and the considered value for the gas constant was $8.314\,51\text{ J mol}^{-1}\text{ K}^{-1}$.²¹ The vapor pressure of water was calculated using the Wagner and Pruss equation of state.²²

The second virial coefficients for pure water and pure hexafluoroethane were taken from the compilation by Dymond and Smith.²³ The crossed virial coefficient for the system water/hexafluoroethane was taken as the arithmetic mean of the second virial coefficients for the two pure substances.

The partial molar volume for hexafluoroethane dissolved in water was calculated, as a function of temperature, using the method described by Toppel and Gubbins^{24,25} which is based on a first-order perturbation theory. The method has been applied to calculate the partial molar volume of several gases in water and proved to be accurate to within 3%.²⁵ This level of uncertainty in the partial molar volume of the solute affects negligibly our values of the Henry's law coefficients (an error of approximately 0.03% in the Henry's law coefficient is obtained for a 10% variation on V_2^{∞}). The partial molar volume at infinite dilution for hexafluoroethane in water, as given by the Toppel and Gubbins method,^{24,25} can be expressed as a function of temperature between 285 and 330 K as

$$\ln(V_2^{\infty}/\text{cm}^3\text{ mol}^{-1}) = 4.350 - 1.51 \times 10^{-4}t \quad (7)$$

where $t = T/K - 273.15$.

Table 1 shows the experimental Henry's law coefficients $H_{2,1}(p_1^{\text{sat}}, T)$ for hexafluoroethane in water from 287 to 328 K. For each point, the temperature and pressure at equilibrium are indicated.

Several empirical methods have been reported in the literature to represent the temperature dependence of Henry's law coefficients. In the present case, two smoothing equations were

TABLE 2: Coefficients for eqs 8–10 and Average Absolute Deviations of the Different Correlations from the Experimental Data^a

eq 8		eq 9		eq 10	
A_0	+1445.9	B_0	$+1.2421 \times 10^2$	C_0	-85.316
A_1	-1972.3	B_1	-1.0284×10^5	C_1	+21.893
A_2	-1166.7	B_2	$+3.5829 \times 10^7$	C_2	+69.68
A_3	+172.87	B_3	-4.1641×10^9		
AAD	0.18%	AAD	0.15%	AAD	0.9%

^a AAD stands for average absolute deviation.

used where the Henry's law coefficient is treated as a partition constant,² function of either the temperature T , or the inverse temperature $1/T$. Clarke and Glew²⁶ proposed as smoothing equation

$$\ln[H_{2,1}(T, p_1^{\text{sat}})/\text{GPa}] = A_0 + \frac{A_1}{(10^{-2}T/\text{K})} + A_2 \ln(10^{-2}T/\text{K}) + A_3 (10^{-2}T/\text{K}) + A_4 (10^{-2}T/\text{K})^2 + \dots \quad (8)$$

whereas Benson and Krause²⁷ fit the experimental values of the Henry's law coefficient to a power series in $1/T$:

$$\ln[H_{2,1}(T, p_1^{\text{sat}})/\text{GPa}] = \sum_{i=0}^n B_i (T/\text{K})^{-i} \quad (9)$$

If the data are to be extrapolated with relative confidence to higher temperatures, it is preferable to use semiempirical correlations that behave correctly even when the critical temperature of the solvent is approached.²⁸ Having this in mind, the experimental results were also fit by eq 10 originally proposed by Harvey:²⁹

$$\ln[H_{2,1}(T, p_1^{\text{sat}})/\text{GPa}] = \ln p_1^{\text{sat}} + \frac{C_0}{T^*} + \frac{C_1(1 - T^*)^{0.355}}{T^*} + C_2 \exp(1 - T^*)(T^*)^{-0.41} \quad (10)$$

where $T^* = T/T_1^{\text{C}}$ and T_1^{C} is the critical temperature of the solvent.

The coefficients A_i , B_i , and C_i for the different correlations used, as well as the average absolute deviations obtained in each case, are listed in Table 2. The average absolute deviations of the fits using eqs 8 and 9 characterize the precision of the experimental results which is of 0.17%. Equation 10 shows a larger average absolute deviation as expected for a less flexible function whose main purpose is to provide a reliable means of extrapolation.^{28,29}

Thermodynamic Functions. The exact expression for the change in partial molar Gibbs energy when the solute is transferred, at temperature T , from the pure perfect gas state at standard pressure to the infinitely dilute state in the solvent (standard Gibbs energy of solvation²⁸) is¹⁹

$$\Delta G_2^0(T, p_1^{\text{sat}}) = RT \ln \left(\frac{H_{2,1}(T, p_1^{\text{sat}})}{p^0} \right) \quad (11)$$

where p_1^{sat} is the saturation pressure of the pure solvent at temperature T and p^0 is the standard pressure. The differences in partial molar enthalpy and entropy between the two states can be obtained by calculating the correspondent partial derivatives of the Gibbs energy with respect to temperature at

TABLE 3: Partial Molar Thermodynamic Functions of Solution for Hexafluoroethane in Water at Several Temperatures between 287 and 328 K^a

<i>T</i> /K	ΔG_2^0 /kJmol ⁻¹	ΔH_2^0 /kJmol ⁻¹	ΔS_2^0 /Jmol ⁻¹ K ⁻¹	ΔCp_2^0 /Jmol ⁻¹ K ⁻¹
288.15	31.784	-37.98	-242.1	1418
293.15	32.938	-31.25	-219.0	1274
298.15	33.980	-25.24	-198.6	1130
303.15	34.927	-19.95	-181.0	987
313.15	36.592	-11.52	-153.7	699
323.15	38.035	-5.96	-136.2	412
328.15	38.700	-4.26	-131.0	269

^a ΔG_2^0 is the partial molar Gibbs energy, ΔH_2^0 is the partial molar enthalpy, ΔS_2^0 is the partial molar entropy, and ΔCp_2^0 is the partial molar isobaric heat capacity. The values refer to the ideal gas state at 101325 Pa.

constant pressure.¹⁹ The result for the enthalpy of solution at temperature *T* and at the pure solvent saturation pressure is

$$\Delta H_2^0(T, p_1^{\text{sat}}) = -RT^2 \left[\frac{d}{dT} \left(\frac{\ln H_{2,1}(T, p_1^{\text{sat}})}{p^0} \right) - \frac{V_2^\infty(T)}{RT} \left(\frac{dp_1^{\text{sat}}(T)}{dT} \right) \right] \quad (12)$$

The difference in partial molar entropy is given by

$$\Delta S_2^0(T, p_1^{\text{sat}}) = -R \left(\frac{\ln H_{2,1}(T, p_1^{\text{sat}})}{p^0} \right) - RT \frac{d}{dT} \left(\frac{\ln H_{2,1}(T, p_1^{\text{sat}})}{p^0} \right) - V_2^\infty(T) \left(\frac{dp_1^{\text{sat}}(T)}{dT} \right) \quad (13)$$

A similar treatment can be adopted to calculate the partial molar heat capacity at constant pressure by taking the partial derivative with respect to temperature, at constant pressure, of the partial molar enthalpy of solution.¹⁹

The values for the different partial molar thermodynamic functions of solution of hexafluoroethane in water were calculated from the values of the smoothing equation proposed by Clarke and Glew, eq 8, and are listed in Table 3. The values presented are relative to the ideal gas state at 101 325 Pa. Krause and Benson made a detailed error analysis²⁷ of this type of procedure to calculate the derived properties from Henry's law coefficients. They compared their values for the thermodynamic functions, calculated using the method described above, with data measured directly by calorimetric techniques³⁰ and concluded that the results agree to within the combined uncertainties for the systems studied (several noble gases in water). The same error analysis was not performed for the present data (no calorimetric values were found for comparison), but the calculation procedure being similar to that described in the literature,^{14,27} the results obtained for the thermodynamic functions are believed to be accurate.

Molecular Simulation

Henry's law coefficients of low molecular weight alkanes and perfluoroalkanes in water were calculated from molecular simulation, over a wide temperature range at conditions close to the saturation line of the pure solvent. Widom's test particle insertion method was used to calculate the chemical potential of the solutes when possible, because it is a simple and exact procedure. It requires the calculation of the interaction energy of a ghost molecule inserted in configurations of the pure solvent, generated, in the present work, by Monte Carlo simulations in the isothermal–isobaric (*NpT*) ensemble. The test

particle insertion method yields values for the residual chemical potential of the solute at infinite dilution, a quantity that can be directly related to the Henry's law coefficient:^{10,31}

$$H_{2,1}(p_1^{\text{sat}}, T) = \lim_{x_2 \rightarrow 0} [RT\rho_1 \exp(\mu^r/RT)] \quad (14)$$

where μ^r is the residual chemical potential of the solute and ρ_1 is the molar density of the pure solvent in the same conditions. The residual chemical potential of the solute is defined as the difference between its chemical potential in solution at a given temperature, density, and composition and the chemical potential of the same species considered as a pure ideal gas at the same temperature and density as in the mixture.

The test particle insertion method works best for solutes of small molecular size and solvents not too dense. Otherwise, the probability of insertion without overlaps between molecules becomes negligible, and the method will suffer from poor statistics. This situation was verified in the present work for the two perfluorinated solutes at the lowest temperatures, and in these cases, an alternative route to calculate the chemical potential was employed, on the basis of the free energy perturbation and thermodynamic integration techniques.³²

Intermolecular Potential Models. Simulations of pure water were performed using simple intermolecular potential models that treat the water molecule as one Lennard-Jones site located on the oxygen atom plus two positive partial charges located on fixed positions corresponding to the hydrogen atoms. One negative partial charge is located either at the center of the oxygen atom (three-site models) or on the dichotomy of the H–O–H angle (four-site model). Several different intermolecular potentials were tried for water in the present work, namely, SPC/E,³³ MSPC/E¹⁰ (three-sites), and TIP4P³⁴ (four-sites). These different models were used in the calculation of the chemical potential of methane and ethane in water and, having observed that all lead to approximately the same results, calculations proceeded using the three-site model SPC/E.

All of the solute molecules (methane, ethane, tetrafluoromethane, and hexafluoroethane) considered in the present study were modeled using united-atom representations in which the sites interact through the Lennard-Jones potential. For the alkanes, the TraPPE parameter set⁷ was used. For hexafluoroethane, the potential parameters proposed by Cui et al.⁶ for sites –CF₃ were considered. These authors developed potential models for longer chain perfluoroalkanes, including site–site parameters for groups –CF₃ and –CF₂– and intramolecular force fields, but they did not study CF₄. Therefore, parameters for tetrafluoromethane were taken from the work of Wen and Muccitelli.⁵

Thus, the molecular models for the solvent and solutes share the same functional form for the site–site interaction energy, given by

$$u(r_{ij}) = 4\epsilon_{ij} \left[\left(\frac{\sigma_{ij}}{r_{ij}} \right)^{12} - \left(\frac{\sigma_{ij}}{r_{ij}} \right)^6 \right] + \frac{q_i q_j}{r_{ij}} \quad (15)$$

and the standard Lorentz–Berthelot combining rules (arithmetic mean for the site diameter, σ , and geometric mean for interaction well depth, ϵ) were used for the interactions between unlike sites. In Table 4, the values for σ , ϵ , and q (partial charge on the hydrogens) as well as the molecular geometries (O–H distance and H–O–H angle) are listed for the SPC/E intermolecular potential for water and also for the models representing the solutes.

Simulation Procedure. The residual chemical potential of the different solutes, except for the perfluoroalkanes at the lowest

TABLE 4: Parameters for the Intermolecular Potential Models Used

	H ₂ O SPC/E ³³	CH ₄ TraPPE ⁷	C ₂ H ₆ TraPPE ⁷	CF ₄ united atom ⁵	C ₂ F ₆ united atom ⁶
$\epsilon/\text{kJ mol}^{-1}$	0.649	1.231	0.815	1.266	0.657
$\sigma/\text{\AA}$	3.166	3.73	3.75	4.70	4.60
$R_{\text{O-H}}/\text{\AA}$	1.0				
$\angle_{\text{H-O-H}}/\text{deg}$	109.47				
q/e	0.4238				
$r_{\text{C-C}}/\text{\AA}$			1.54		1.54

temperatures, was calculated using Widom's test particle insertion method.³⁵ All of the computer simulation programs used were written by the authors.

Pure liquid water was initially simulated by the Monte Carlo method in the NpT ensemble using cubic periodic boundary conditions. For this purpose, initially 256 water molecules and later 500 and 1372 molecules were equilibrated during $(10-50) \times 10^3$ simulation cycles (one cycle is composed of N attempts to displace or rotate a molecule chosen at random plus one attempt to change the volume of the system in order to keep the pressure constant), depending on the temperature. Then, another 100×10^3 simulation cycles were performed to collect averages for the thermodynamic properties. From each of these simulations of water, 1000 configurations were stored to be used in the calculation of the residual chemical potential of the different solutes by test particle insertion.

The cutoff radius for the water–water interaction was established at 9 Å and the same value was adopted for the solute–solvent interactions in the case of methane and ethane. A larger truncation radius of 12 Å was used for the fluorinated solutes. Corrections for the truncation of the Lennard-Jones potential beyond the cutoff radius were calculated by integration of the energy and virial equations.³⁶ The long-range electrostatic interactions in water were taken into account using the Ewald summation method, extending the reciprocal space sum to a number of eight wave vectors and using a value of 0.35 for the parameter κ ³⁶ that controls the width of the screening Gaussian charge distribution.

According to the test particle insertion method, the residual chemical potential μ^r is evaluated from the expression³⁶

$$\mu_2^r = -kT \frac{\langle V \exp(u_{\text{TP}}/kT) \rangle_{NpT}}{\langle V \rangle_{NpT}} \quad (16)$$

in which u_{TP} is the interaction energy of the test particle with a configuration of solvent molecules, V is the volume of the solvent in a given configuration and $\langle \dots \rangle_{NpT}$ denotes an isothermal–isobaric ensemble average. The chemical potential was calculated by averaging over $(40-200) \times 10^3$ test particle insertions per configuration of solvent, depending on the temperature and on the size of the solute molecule. For methane and ethane, insertions in configurations of 256 water molecules proved sufficient to yield good statistics for the chemical potential. On the other hand, a larger number of water molecules, 500 at least, had to be simulated in order to accommodate the larger cutoff radius employed for the perfluoroalkane–water interactions.

When the direct test particle insertion method yields poor statistics, free energy differences and chemical potentials (which are analogous to free energy differences associated with the addition of one molecule to an infinitely large system) can be obtained following a number of routes.³² Standard methods such as free energy perturbation and thermodynamic integration require the construction of a path connecting the Hamiltonian

of an initial system (for example the pure solvent) to that of the final system (one solute molecule interacting with the solvent). Several steps of free energy perturbation, or several points along a thermodynamic integration path, have to be used when the initial and final systems sample distant regions in configurational space.³⁷ Because in our application the test particle method produced good results for the chemical potential of methane and ethane, we decided to evaluate the free energy difference corresponding to the transformation of one alkane molecule into the corresponding perfluoroalkane molecule. This smaller step requires less computation effort and produces smaller overall uncertainties than the alternative activation of an entire solute molecule starting from the pure solvent. A path connecting the intermolecular potential of the alkane and the perfluoroalkane was established according to

$$\begin{aligned} \sigma(\lambda) &= \lambda \sigma_{\text{CF}_x} + (1 - \lambda) \sigma_{\text{CH}_x} \\ \epsilon(\lambda) &= \lambda \epsilon_{\text{CF}_x} + (1 - \lambda) \epsilon_{\text{CH}_x} \end{aligned} \quad (17)$$

where the activation parameter λ varies from 0 to 1. Conveniently, the carbon–carbon distance in both the TraPPE ethane model and in the model for hexafluoroethane are identical, as can be seen in Table 4. The technique chosen to evaluate the free energy differences is the finite-difference thermodynamic integration (FDTI) method, which uses the thermodynamic integration formula

$$\Delta G = \int_0^1 \frac{\partial G}{\partial \lambda} d\lambda = \int_0^1 \left\langle \frac{\partial H}{\partial \lambda} \right\rangle_{\lambda} d\lambda \quad (18)$$

to evaluate ΔG , and the free energy perturbation method to evaluate the derivative at each value of λ :

$$\frac{\partial G}{\partial \lambda} \approx -kT \frac{\ln \langle V \exp[-(H(\lambda + \delta\lambda) - H(\lambda - \delta\lambda))/kT] \rangle_{NpT}}{2\delta\lambda \langle V \rangle_{NpT}} \quad (19)$$

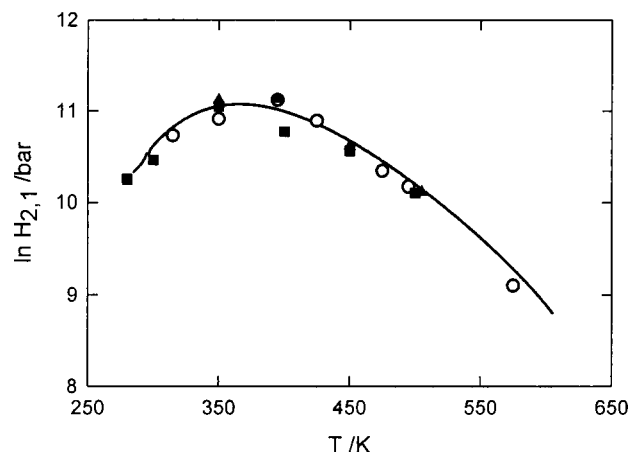
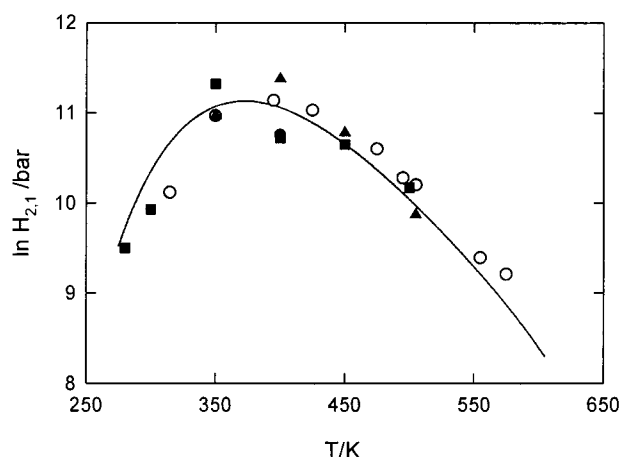
where δ is a small increment (of the order of 0.001) used to calculate the central three-point numerical derivative. Six points were obtained along the paths corresponding to the transformation of a methane molecule into one of tetrafluoromethane, and of an ethane molecule into one of hexafluoroethane, at values of $\lambda = 0.0, 0.2, 0.4, 0.6, 0.8$, and 1.0. At each value of the coupling parameter, systems containing one solute molecule and 500 water molecules were simulated during 60×10^3 Monte Carlo cycles after equilibration. The results for the free energy differences agree totally with those calculated using the free energy perturbation technique for the same path, although this last method showed small hystereses (at most 0.3 kJ mol^{−1}) when growing from the alkane to the fluorinated alkane or following the reverse route. The values for the chemical potential obtained from this combination of test particle insertion with FDTI are also in accord with tests using the free energy perturbation method to perform a staged insertion of an hexafluoroethane molecule in water starting from the pure solvent.

Simulation Results. Simulation results for the Henry's law coefficients of the different solutes in water are reported in Table 5. The values obtained for the density of water are coherent with the intermolecular potential model considered.²⁹ The statistical uncertainties associated with the values of fluctuating properties were calculated using the block average procedure.³⁶

Figures 2 and 3 show the simulated Henry's law coefficients of methane and ethane in water, with all values having been obtained by the test particle insertion method. The calculations

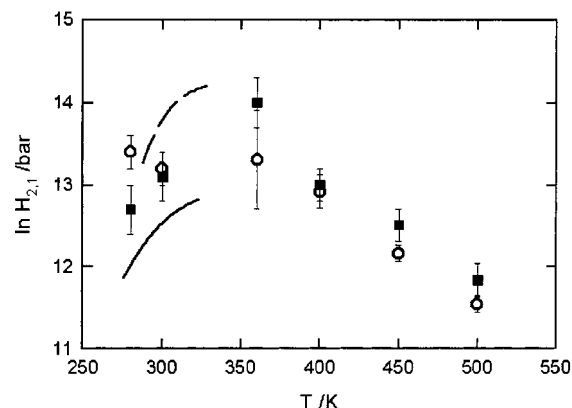
TABLE 5: Simulation Results for the Density of Water (NpT Ensemble Monte Carlo with SPC/E Model for Water) and for the Henry's Law Coefficients of the Different Solutes in Water

T/K	280	300	360	400	450	500
p/MPa	0.02	0.03	0.40	2.50	9.30	26.0
$\rho_{\text{H}_2\text{O}}/\text{mol dm}^{-3}$	55.69 ± 0.18	55.29 ± 0.15	52.94 ± 0.10	50.77 ± 0.10	47.65 ± 0.11	44.00 ± 0.14
$\mu^E(\text{CH}_4)/\text{kJ mol}^{-1}$	7.2 ± 0.3	8.04 ± 0.20	11.0 ± 0.3	11.11 ± 0.20	11.48 ± 0.12	10.66 ± 0.21
$\ln[H_{2,1}(\text{CH}_4)/\text{bar}]$	10.24 ± 0.13	10.45 ± 0.08	11.03 ± 0.09	10.77 ± 0.06	10.55 ± 0.03	10.08 ± 0.05
$\mu^E(\text{C}_2\text{H}_6)/\text{kJ mol}^{-1}$	5.4 ± 0.5	6.7 ± 0.3	11.5 ± 0.3	11.0 ± 0.4	11.8 ± 0.3	10.9 ± 0.3
$\ln[H_{2,1}(\text{C}_2\text{H}_6)/\text{bar}]$	9.50 ± 0.20	9.93 ± 0.14	11.22 ± 0.11	10.73 ± 0.11	10.64 ± 0.07	10.15 ± 0.08
$\mu^E(\text{CF}_4)/\text{kJ mol}^{-1}$	14.6 ± 0.5	14.9 ± 0.4	17.7 ± 1.8	18.3 ± 0.6	17.5 ± 0.4	16.8 ± 0.4
$\ln[H_{2,1}(\text{CF}_4)/\text{bar}]$	13.4 ± 0.2	13.2 ± 0.2	13.3 ± 0.6	12.9 ± 0.2	12.2 ± 0.1	11.6 ± 0.1
$\mu^E(\text{C}_2\text{F}_6)/\text{kJ mol}^{-1}$	12.9 ± 0.7	14.6 ± 0.5	19.8 ± 1.0	18.5 ± 0.6	18.7 ± 0.9	17.9 ± 0.8
$\ln[H_{2,1}(\text{C}_2\text{F}_6)/\text{bar}]$	12.7 ± 0.3	13.1 ± 0.3	14.0 ± 0.3	13.0 ± 0.2	12.5 ± 0.2	11.8 ± 0.2

**Figure 2.** Henry's law coefficients of methane in water. (—) Correlation of experimental results;²³ (○) simulation data of Errington et al.;³⁸ (●) this work, MSPC/E model for water; (▲) this work, TIP4P model for water; (■) this work, SPC/E model for water.**Figure 3.** Henry's law coefficients of ethane in water. (—) Correlation of experimental results;²³ (○) simulation data of Errington et al.;³⁸ (●) this work, MSPC/E model for water; (▲) this work, TIP4P model for water; (■) this work, SPC/E model for water.

of the present work using different intermolecular potentials for water are compared with those by Errington et al.³⁸ and with the correlation of experimental data published by Harvey.²⁹ Our results are in good agreement with the correlation and seem insensitive to the intermolecular potential model adopted for water. The behavior with temperature along the saturation line of the solvent is correctly predicted.

The fluorinated molecules are larger than the corresponding alkanes, and their chemical potentials are more difficult to obtain by test particle insertion, especially at lower temperatures because of the higher solvent density, as evidenced by the larger

**Figure 4.** Henry's law coefficients of tetrafluoromethane and hexafluoroethane in water. (—) Experimental results for CF_4 of Scharlin and Battino;⁴⁰ (—) experimental results for C_2F_6 , this work; (○) simulation results for CF_4 in water, this work; (●) simulation results for C_2F_6 in water, this work.

uncertainties affecting the calculated Henry's law coefficients, particularly at 360 K. Tests were performed using 1372 water molecules in order to better represent the solvent configurational space. However, no significant improvements were detected in the values of the final residual chemical potential. At the two lowest temperatures, the statistical uncertainties prevent a reliable determination of this quantity from test particle insertion. The values reported in Table 5 for the fluorinated solutes at 280 and 300 K were calculated by the FDTI method as described above.

The Henry's law coefficients of the two perfluoroalkanes obtained from simulation are plotted in Figure 4. Experimental data for comparison are available only up to 330 K. It is observed that the Henry's law coefficients are predicted qualitatively although the solubility difference between both solutes is not reproduced by the simulations. This deficiency is not uniquely related to statistical errors but is a consequence of the intermolecular potential models. Over a wide temperature range, the nonmonotonic temperature dependence of $H_{2,1}$ is reproduced by the simulations.

The solute-solvent site-site radial distribution functions were also obtained by simulating systems containing one solute molecule among 500 water molecules, at 300 and 450 K. After equilibrating, simulations of 100×10^3 cycles were conducted to accumulate histograms for the different site-site radial distribution functions. The results are depicted in Figure 5. At 300 K, the first maxima of $g_{i-\text{OW}}$ and $g_{i-\text{HW}}$ (where i is one of the solute sites) coincide, indicating the tangential orientation of the water molecules in the first solvation shell, as expected for nonpolar solutes in water. The shoulder observed on the first peak of $g_{i-\text{HW}}$, more evident for CH_4 and CF_4 , is also characteristic of these interactions. Increasing the temperature

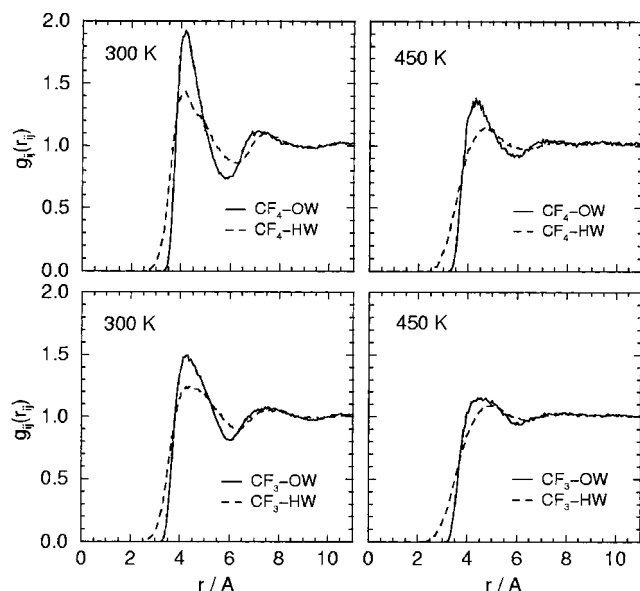


Figure 5. Radial distribution functions for the different solutes in water at 300 and 450 K. The site-site function $g_{i-OW}(r)$ represents the distribution of oxygen atoms from water around site i of the solutes, whereas $g_{i-HW}(r)$ gives the distribution of hydrogen atoms from water around site i of the solutes.

brings the usual decrease in amplitude of the oscillations of the radial distribution functions. The first peak of g_{i-HW} is now shifted to larger distances when compared to the first peak in g_{i-OW} , indicating the preferential orientation of the hydrogen atoms toward the bulk of the solvent.³⁹

Conclusions

The present paper reports new, highly accurate experimental results of solubility of hexafluoroethane in water, which are original above 303 K. These measurements are particularly difficult because the solubility of perfluoroalkanes in water is very low. The temperature range studied, together with the high precision of the data, allows the derivation of several important thermodynamic quantities characteristic of the dissolution process that up to now had not been determined directly.

Computer simulation was employed as a predictive tool, using intermolecular potential models taken from the literature. The choice of united-atom models for perfluoroalkanes seems to be a good option for the macroscopic properties and systems studied, providing reasonable agreement with experimental data. The methods adopted to calculate the residual chemical potential of the solutes in water, and from there Henry's law coefficients and solubilities, proved adequate and efficient for the solutes in question over a large temperature range. Simple, unbiased test particle insertions produced precise enough results for all of the solutes studied except for the perfluoroalkanes at the low-temperature end, where large statistical uncertainties were obtained. In these conditions, a finite-difference thermodynamic integration method was implemented. The correct, nonmonotonic temperature dependence of the Henry's law coefficients is well reproduced.

The Henry's law constants, being a property at infinite dilution, depend on the solute-solvent interactions and not on those present in the pure solute. This aspect may contribute to improve interaction models for mixtures. However, we show that to a first approximation simple combining rules, applied to intermolecular potentials developed for the pure solvent and pure solute separately, yield reasonable results, following a purely predictive scheme. The combined approach of the present

work demonstrates that computer simulation can serve as a complement to experimental measurements allowing us to extend the ranges of conditions where data are available and providing a reliable means of extrapolation.

References and Notes

- (1) Johnston, K. P.; Harrison, K. L.; Clarke, M. J.; Howdle, S. M.; Heitz, M. P.; Bright, F. V.; Carlier, C.; Randolph, T. W. *Science* **1996**, 271, 624.
- (2) McClain, J. B.; Betts, D. E.; Canelas, D. A.; Samulski, E. T.; DeSimone, J. M.; Londono, J. D.; Cochran, H. D.; Wignall, G. D.; Chillura-Martino, D.; Triolo, R. *Science* **1996**, 274, 2049.
- (3) Wilhelm, E. *CRC Crit. Rev. Anal. Chem.* **1985**, 16, 129.
- (4) Swinton, S. L. In *Chemical Thermodynamics*; McGlashan, M. L., Ed.; The Chemical Society: London, 1978; Vol. 2, pp 147-173.
- (5) Hildebrand, J. H.; Prausnitz, J. M.; Scott, R. L. *Regular and Related Solutions*; Van Nostrand Reinhold Co.: New York, 1970; pp 111-141.
- (6) Wen, W.-Y.; Muccitelli, J. A. *J. Solution Chem.* **1979**, 8, 225.
- (7) Cui, S. T.; Siepmann, J. I.; Cochran, H. D.; Cummings, P. T. *Fluid Phase Equilibria* **1998**, 146, 51.
- (8) Martin, M. G.; Siepmann, J. I. *J. Phys. Chem. B* **1998**, 102, 2569.
- (9) Toxvaerd, S. *J. Chem. Phys.* **1997**, 107, 5197.
- (10) Potter, S. C.; Tildesley, D. J.; Burgess, A. N.; Rogers, S. C. *Mol. Phys.* **1997**, 92, 825.
- (11) Boulougouris, G. C.; Economou, I. G.; Theodorou, D. N. *J. Phys. Chem. B* **1998**, 102, 1029.
- (12) Costa Gomes, M. F.; Grolier, J.-P. *Phys. Chem. Chem. Phys.* **2001**, 3, 1047.
- (13) Benson, B. B.; Krause, D., Jr.; Peterson, M. A. *J. Solution Chem.* **1979**, 8, 655.
- (14) Benson, B. B.; Krause, D., Jr. *J. Phys. Chem.* **1976**, 80, 689.
- (15) Rettich, T. R.; Paul Handa, Y.; Battino, R.; Wilhelm, E. *J. Phys. Chem.* **1981**, 85, 3230.
- (16) Rettich, T. R.; Battino, R.; Wilhelm, E. *Ber. Bunsen-Ges. Phys. Chem.* **1982**, 86, 1128.
- (17) Rettich, T. R.; Battino, R.; Wilhelm, E. *J. Solution Chem.* **1992**, 21, 987.
- (18) Rettich, T. R.; Battino, R.; Wilhelm, E. *J. Chem. Thermodyn.* **2000**, 32, 1145.
- (19) Battino, R.; Banzhof, M.; Bogan, M.; Wilhelm, E. *Anal. Chem.* **1971**, 43, 806.
- (20) Smith, J. M.; Van Ness, H. C.; Abbott, M. M. *Introduction to Chemical Engineering Thermodynamics*, 5th ed.; McGraw-Hill: New York, 1996.
- (21) IUPAC, Commission on Atomic Weights and Isotopic Abundances, *Pure Appl. Chem.* **1986**, 58, 1677.
- (22) IUPAC, *Quantities, Units and Symbols in Physical Chemistry*; Blackwell Scientific Publications: Oxford, U.K., 1988.
- (23) Wagner, W.; Pruss, A. *J. Phys. Chem. Ref. Data* **1993**, 22, 783.
- (24) Dymond, J. H.; Brian Smith, E. *The Virial Coefficients of Pure Gases and Mixtures*; Oxford University Press: Oxford, U.K., 1980.
- (25) Toppel, E. W.; Gubbins, K. E. *Can. J. Chem. Eng.* **1972**, 50, 361.
- (26) Toppel, E. W.; Gubbins, K. E. *J. Phys. Chem.* **1972**, 76, 3044.
- (27) Clarke, E. C. W.; Glew, D. N. *Trans. Faraday Soc.* **1966**, 62, 539.
- (28) Krause, D.; Benson, B. B. *J. Solution Chem.* **1989**, 18, 823.
- (29) Harvey, A. H.; Levelt Sengers, J. M. H.; Tanger, J. C., IV. *J. Phys. Chem.* **1991**, 95, 932.
- (30) Harvey, A. H. *AIChE J.* **1996**, 42, 1491.
- (31) Dec, S. F.; Gill, S. J. *J. Solution Chem.* **1984**, 13, 27.
- (32) Lee, L. L. *Molecular Thermodynamics of Nonideal Fluids*; Butterworth: Boston, MA, 1988.
- (33) Kollman, P. *Chem. Rev.* **1993**, 9, 2395.
- (34) Berendsen, H. J. C.; Greijera, J. R.; Straatsma, T. P. *J. Phys. Chem.* **1987**, 91, 6269.
- (35) Jorgensen, W. L.; Chandrasekhar, J.; Madura, J. D.; Impey, R. W.; Klein, M. L. *J. Chem. Phys.* **1983**, 79, 926.
- (36) Widom, B. *J. Chem. Phys.* **1963**, 39, 2908.
- (37) Allen, M. P.; Tildesley, D. J. *Computer Simulation of Liquids*; Oxford University Press: Oxford, U.K., 1987.
- (38) Kofke, D. A.; Cummings, P. T. *Mol. Phys.* **1997**, 92, 973.
- (39) Errington, J. R.; Boulougouris, G. C.; Economou, I. G.; Panagiotopoulos, A. Z.; Theodorou, D. N. *J. Phys. Chem. B* **1998**, 102, 8865.
- (40) Guillot, B.; Guissani, Y. *Proc. Int. Conf. Prop. Water Steam*, 12th **1995**, 269-277.
- (41) Scharlin, P.; Battino, R. *J. Chem. Eng. Data* **1995**, 40, 167.